

DANYELLA CAROLYNA SOARES DOS REIS

**CARACTERIZAÇÃO FÍSICO-QUÍMICA E EFEITO BIOLÓGICO DE
SCAFFOLDS 3D-NANOFIBRILARES DE ALUMINA
PRODUZIDOS POR FIAÇÃO POR SOPRO EM SOLUÇÃO.**

Physicochemical characterization and biological effect of 3D-nanofibrous alumina scaffolds produced by solution blow spinning.

Dissertação apresentada à Faculdade de Odontologia da Universidade Federal de Uberlândia, para obtenção do Título de Mestre em Odontologia na Área de Clínica Odontológica Integrada.

Uberlândia, 2021.

DANYELLA CAROLYNA SOARES DOS REIS

**CARACTERIZAÇÃO FÍSICO-QUÍMICA E EFEITO BIOLÓGICO DE
SCAFFOLDS 3D-NANOFIBRILARES DE ALUMINA
PRODUZIDOS POR FIAÇÃO POR SOPRO EM SOLUÇÃO.**

Physicochemical characterization and biological effect of 3D-nanofibrous alumina scaffolds produced by solution blow spinning.

Dissertação apresentada à Faculdade de Odontologia da Universidade Federal de Uberlândia, para obtenção do Título de Mestre em Odontologia na Área de Clínica Odontológica Integrada.

Orientadora: Prof^ª Dr^ª Paula Dechichi

Co-orientadora: Prof^ª Dr^ª Flaviana Soares Rocha

Banca examinadora:

Prof^ª Dr^ª Paula Dechichi

Prof. Dr. Jonas Dantas Batista

Prof. Dr. Romualdo Rodrigues Meneses

Uberlândia, 2021.



UNIVERSIDADE FEDERAL DE UBERLÂNDIA
 Coordenação do Programa de Pós-Graduação em Odontologia
 Av. Pará, 1720, Bloco 4L, Anexo B, Sala 33 - Bairro Umusarama, Uberlândia-MG, CEP 38400-902
 Telefone: (34) 3225-8115/8108 - www.ppgoufu.com - copod@umusarama.ufu.br



ATA DE DEFESA - PÓS-GRADUAÇÃO

| | | | | | |
|------------------------------------|---|-----------------|-------|-----------------------|-------|
| Programa de Pós-Graduação em: | Odontologia | | | | |
| Defesa de: | Dissertação de Mestrado Acadêmico. número 393, PPGODONTO | | | | |
| Data: | Vinte e Seis de Julho de Dois Mil e Vinte e Um | Hora de início: | 09:00 | Hora de encerramento: | 11:30 |
| Matrícula do Discente: | 11912000006 | | | | |
| Nome do Discente: | Danyella Carolyn Soares dos Reis | | | | |
| Título do Trabalho: | Caracterização físico-química e efeito biológico de scaffolds 3D nanofibrilares de alumina produzidos por fiação por sopro em solução | | | | |
| Área de concentração: | Clínica Odontológica Integrada | | | | |
| Linha de pesquisa: | Processo de Reparo | | | | |
| Projeto de Pesquisa de vinculação: | Processo de Reparo | | | | |

Reuniu-se em Web Conferência pela plataforma Zoom, em conformidade com a PORTARIA Nº 36, DE 19 DE MARÇO DE 2020 da COORDENAÇÃO DE APERFEIÇOAMENTO DE PESSOAL DE NÍVEL SUPERIOR - CAPES, pela Universidade Federal de Uberlândia, a Banca Examinadora, designada pelo Colegiado do Programa de Pós-graduação em Odontologia, assim composta: Professores Doutores: Jonas Dantas Batista (UFU); Romualdo Rodrigues Menezes (UFCG); Paula Dechichi Barbar (UFU) orientadora da candidata.

Iniciando os trabalhos a presidente da mesa, Dra. Paula Dechichi Barbar, apresentou a Comissão Examinadora e o candidato(a), agradeceu a presença do público, e concedeu ao Discente a palavra para a exposição do seu trabalho. A duração da apresentação do Discente e o tempo de arguição e resposta foram conforme as normas do Programa.

A seguir o senhor(a) presidente concedeu a palavra, pela ordem sucessivamente, aos(às) examinadores(as), que passaram a arguir o(a) candidato(a). Ultimada a arguição, que se desenvolveu dentro dos termos regimentais, a Banca, em sessão secreta, atribuiu o resultado final, considerando o(a) candidato(a):

Aprovada.

Esta defesa faz parte dos requisitos necessários à obtenção do título de Mestre.

O competente diploma será expedido após cumprimento dos demais requisitos, conforme as normas do Programa, a legislação pertinente e a regulamentação interna da UFU.

Nada mais havendo a tratar foram encerrados os trabalhos. Foi lavrada a presente ata que após lida e achada conforme foi assinada pela Banca Examinadora.



Documento assinado eletronicamente por Paula Dechichi Barbar, Professor(a) do Magistério Superior, em 26/07/2021, às 11:35, conforme horário oficial de Brasília, com fundamento no art. 6º, § 1º, do [Decreto nº 8.539, de 8 de outubro de 2015](#).



Documento assinado eletronicamente por Jonas Dantas Batista, Professor(a) do Magistério Superior, em 26/07/2021, às 11:36, conforme horário oficial de Brasília, com fundamento no art. 6º, § 1º, do [Decreto nº 8.539, de 8 de outubro de 2015](#).



Documento assinado eletronicamente por Romualdo Rodrigues Menezes, Usuário Externo, em 26/07/2021, às 11:37, conforme horário oficial de Brasília, com fundamento no art. 6º, § 1º, do [Decreto nº 8.539, de 8 de outubro de 2015](#).



A autenticidade deste documento pode ser conferida no site https://www.sei.ufu.br/sei/controlador_externo.php?acao=documento_conferir&id_orgao_acesso_externo=0, informando o código verificador 2918212 e o código CRC 0B4804CF.

Ficha Catalográfica Online do Sistema de Bibliotecas da UFU
com dados informados pelo(a) próprio(a) autor(a).

| | |
|--------------|--|
| R375 2021 | Reis, Danyella Carolyn Soares dos, 1995- CARACTERIZAÇÃO FÍSICO-QUÍMICA E EFEITO BIOLÓGICO DE SCAFFOLDS 3D-NANOFIBRILARES DE ALUMINA PRODUZIDOS POR FIAÇÃO POR SOPRO EM SOLUÇÃO. [recurso eletrônico] / Danyella Carolyn Soares dos Reis. - 2021. Orientadora: Paula Dechichi . Coorientadora: Flaviana Soares Rocha. Dissertação (Mestrado) - Universidade Federal de Uberlândia, Pós-graduação em Odontologia. Modo de acesso: Internet. Disponível em: http://doi.org/10.14393/ufu.di.2021.346 Inclui bibliografia. 1. Odontologia. I. , Paula Dechichi, 1965-, (Orient.). II. Rocha, Flaviana Soares, 1986-, (Coorient.). III. Universidade Federal de Uberlândia. Pós-graduação em Odontologia. IV. Título. CDU: 616.314 |
|--------------|--|

Bibliotecários responsáveis pela estrutura de acordo com o AACR2:

Gizele Cristine Nunes do Couto - CRB6/2091

AGRADECIMENTOS

Agradeço, primeiramente, a Deus por tudo que conquistei até aqui, e peço sabedoria para conquistar mais. Em segundo lugar agradeço aos meus pais e minhas irmãs que tornaram essa caminhada mais fácil, sendo meu apoio e sustento.

Ao meu amor Everton, obrigada pela paciência, pelo companheirismo, pelo incentivo e pelas horas dos fins de semana que sacrificou para me ajudar.

Muito obrigada às minhas orientadoras Prof. Dr^a Flaviana Soares Rocha e Prof. Paula Dechichi pela oportunidade de participar deste trabalho, pelo carinho, apoio, atenção e paciência.

À minha amiga e braço direito nesses dois anos e meio, Rita Catarina, muito obrigada por me aguentar e ajudar a compartilhar o fardo de quando tudo dava errado.

À equipe que me auxiliou nas etapas experimentais, Camila Linhares, Pedro Limirio, Jessyca Venancio, Marcelo Dias, Luiz Henrique, muito obrigada, vocês foram fundamentais.

Obrigada!

SUMÁRIO

| | |
|-------------------------------------|----|
| LISTA DE ABREVIATURAS | 5 |
| RESUMO/PALAVRAS-CHAVE | 6 |
| ABSTRACT/KEYWORDS | 7 |
| 1. INTRODUÇÃO E REFERENCIAL TEÓRICO | 8 |
| 2. CAPÍTULO ÚNICO – ARTIGO | 11 |
| 3. CONCLUSÃO | 26 |
| REFERÊNCIAS BIBLIOGRÁFICAS | 27 |
| ANEXO 1 | 32 |

LISTA DE ABREVIATURAS

SBS – solution blow spinning / fiação por sopro em solução

PVP – polivinilpirrolidona

3D – tridimensional

MEV/SEM – microscopia eletrônica de varredura / scanning electron microscopy

DRX/XRD – difração de raios-x / X-ray diffraction

nm – nanômetro

Al₂O₃ – Óxido de alumínio

g - grama

h - hora

g/mol – gramas por mol

ml/h – mililitro por hora

MPa – mega Pascal

°C – graus Celsius

kV – quilovolt

mA – miliampere

mg/kg – miligrama por quilograma

mm – milímetro

PBS - Phosphate-buffered saline

µm – micrometro

HE – Hematoxilina e Eosina

MT – Tricromio de Mallory

ES – Eletrospinning

α-Al₂O₃ – alfa alumina

γ-Al₂O₃ – gama alumina

RESUMO

Biomateriais substitutos ósseos com potencial para melhorar as interações célula-material estão em alta demanda. O objetivo deste estudo foi caracterização físico-química e avaliação *in vivo* da bioatividade de scaffolds amorfos 3D-nanofibrosos de alumina, produzidos pela técnica de SBS (*Solution Blow Spinning*) para regeneração óssea. As nanofibras utilizadas neste estudo foram obtidas a partir de uma solução de nitrato de alumínio, polivinilpirrolidona (PVP), etanol e água destilada, e fiadas no aparelho de SBS sob pressão e temperatura definidas. As fibras possuíam estrutura macro e microscópica 3D semelhante a algodão e foram calcinadas a 500°C. A caracterização morfológica das nanofibras foi realizada por meio de microscopia eletrônica de varredura (MEV), e a caracterização mineralógica por difração de raios X (DRX). Para avaliar o efeito biológico, defeitos ósseos foram criados no fêmur de 20 ratos Wistar machos. Os defeitos foram preenchidos com sangue ou nanofibras de alumina e os animais foram sacrificados após 14 ou 28 dias. Os fêmures foram coletados e processados para obtenção das lâminas histológicas. Foi realizada análise descritiva histológica do reparo ósseo, associado ao biomaterial. Além disso, a neoformação óssea e as partículas remanescentes do biomaterial foram quantificadas para a análise histomorfométrica. Na análise morfológica, as nanofibras apresentaram secção transversal circular com diâmetros médios de 287nm; o padrão de DRX não apresentou reflexos de difração, caracterizando uma alumina amorfa. A histomorfometria revelou maior quantidade de neoformação óssea nos grupos Alumina quando comparados ao controle nos dois períodos experimentais ($p < 0,05$) e a porcentagem partículas de enxerto de Alumina remanescentes em 14 e 28 dias foi semelhante. Em conclusão, os scaffolds de alumina 3D testados permitiram a deposição óssea e favoreceram que o preenchimento do defeito ósseo com osso novo.

PALAVRAS-CHAVE: Alumina nanofibrosa, scaffold tridimensional, reparo ósseo.

ABSTRACT

Bone substitute biomaterials with the potential to improve cell-material interactions are in high demand. The aim of this study was to perform physicochemical characterization and evaluate *in vivo* the bioactivity of amorphous 3D-nanofibrous alumina scaffolds produced by the SBS (*Solution Blow Spinning*) technique for bone regeneration. The nanofibers used in this study were obtained from a solution of aluminum nitrate, polyvinylpyrrolidone (PVP), ethanol and distilled water, and spun in the SBS apparatus under defined pressure and temperature. The fibers had a macro and microscopic cotton-like 3D structure and were calcined at 500°C. The morphological characterization of the nanofibers was performed using scanning electron microscopy (SEM), and the mineralogical characterization by X-ray diffraction (XRD). To evaluate the biological effect, bone defects were created in the femur of 20 male Wistar rats. The defects were filled with blood or alumina nanofibers. The animals were euthanized at 14 or 28 days. Femurs were collected and processed to obtain histological slides. Descriptive histological analysis of the bone repair process associated with the biomaterial was performed. Also, bone neoformation and the particles of the remaining graft were quantified for histomorphometry analysis. In the morphological analysis, the nanofibers had a circular cross section with mean diameters of 287 nm; the XRD pattern did not present diffraction reflections, characterizing an amorphous alumina. Histomorphometry revealed a greater amount of bone neoformation in the Alumina groups when compared to the control in the two experimental periods ($p < 0.05$) and the percentage of Alumina graft particles remaining at 14 and 28 days was similar. In conclusion, the tested 3D alumina scaffolds allowed bone deposition and favored bone defect filling with new bone.

KEY-WORDS: nanofibrous alumina, three-dimensional scaffold, bone repair.

1. INTRODUÇÃO E REFERENCIAL TEÓRICO

A reconstrução adequada dos defeitos ósseos no complexo maxilomandibular com bons resultados estéticos e funcionais continua sendo um desafio na cirurgia bucal e maxilofacial. Ao longo dos anos, vários métodos têm sido utilizados, tais como enxerto ósseo autógeno livre ou vascularizado, além do concentrado ósseo aspirado de medula óssea, com bons resultados (MELVILLE et al. 2016). No entanto, podem surgir complicações relacionadas aos procedimentos cirúrgicos tais como sangramento, infecção e dor crônica no sítio doador, bem como aumento de custos e tempo operatório (CONWAY, 2010). Como resultado, a demanda por substitutos aos enxertos ósseos autógenos levou à pesquisa multidisciplinar projetada para desenvolver novos biomateriais.

Biomaterial é qualquer substância sintética ou natural que possa ser utilizada para substituição total ou parcial de qualquer tecido ou órgão do organismo (GUASTALDI, 2004). São requisitos desejáveis de um biomaterial, a biocompatibilidade, atoxicidade, não ser carcinogênico ou pirogênico, apresentar estabilidade química e biológica, baixa densidade, resistência mecânica e elástica adequadas, e baixo custo (BOSS et al., 1995; GUASTALDI, 2004). O principal desafio existente nos estudos de biomateriais é encontrar um material que seja o mais parecido possível com o tecido vivo, de modo que o organismo possa reconhecê-lo como parte de sua estrutura e não como um agente agressor ao seu meio.

Para a regeneração dos defeitos ósseos de continuidade é interessante desenvolver uma estrutura tridimensional que se assemelhe à microestrutura, composição química e às propriedades mecânicas e funcionais do tecido nativo a ser reconstruído. Tais estruturas são comumente chamadas de *scaffolds* (HEJAZI E MIRZADEH, 2016). Os *scaffolds* devem apresentar resistência mecânica apropriada, biocompatibilidade e biodegradabilidade, permitindo deposição e remodelação óssea na região do defeito. As propriedades dos *scaffolds* dependem principalmente da natureza do biomaterial utilizado, que inclui diferentes origens como metais, cerâmicas, polímeros naturais e

combinação destes com íons visando obtenção de compósitos. (KARAGEORGIU & KAPLAN, 2015; GAO et al., 2014).

Uma das propriedades de interesse de um *scaffold* é a sua porosidade, que é definida como sendo a porcentagem de espaço vazio em um sólido. Os poros são necessários porque permitem a migração e a proliferação de osteoblastos e células mesenquimais, bem como posterior vascularização da região. Além disso, uma superfície porosa melhora o imbricamento mecânico entre o biomaterial e o osso natural envolvente, proporcionando uma maior estabilidade mecânica (KARAGEORGIU & KAPLAN, 2015; VALLET-REGÍ, 2010).

Para a produção de *scaffolds* porosos diversas técnicas podem ser empregadas. As técnicas convencionais incluem a adição de agente de formação de poros em cerâmica e a formação de espuma química. Porém, esses métodos têm baixo controle da estrutura dos poros, resultando em poros de tamanho, conectividade e forma heterogêneos (GAO et al., 2014). Recentemente, *scaffolds* fibrosos, compostos por fibras com diâmetros que variam de dezenas de nanômetros até alguns micrômetros, ganharam destaque, principalmente, devido à semelhança estrutural com a matriz extracelular (ECM) e a disponibilidade de processamento utilizando diversos materiais. Além disso, são técnicas relativamente simples e de baixo custo para sua realização (JUN-HYEOG et al., 2009).

A principal técnica utilizada para produção de *scaffolds* fibrosos é a eletrofiação, considerada uma técnica eficiente na obtenção de fibras com diâmetro variando de 2 nanômetros a vários micrômetros. Entretanto, a eletrofiação apresenta como desvantagens a impossibilidade de produção de fibras em grande quantidade, dificultando seu uso em escala industrial. Mais recentemente foi desenvolvida a técnica denominada *Solution Blow Spinning* (SBS) ou fiação por sopro em solução para produção de *scaffolds* fibrosos (MEDEIROS et al., 2009).

As vantagens do SBS estão relacionadas à possibilidade da produção de fibras micro e nanométricas tridimensionais, em larga escala e com custo

reduzido. Além disso, necessita de um aparato bastante simples para o seu funcionamento, sem a necessidade de equipamento de voltagem para a produção das fibras (BONAN et al., 2015).

Existem inúmeros materiais investigados para utilização como *scaffolds* para substitutos ósseos. Entre os utilizados, estão os materiais metálicos, não metálicos inorgânicos e materiais orgânicos. Várias formas de cerâmica de alumina foram estudadas para diferentes aplicações. Atualmente, a Alumina (Al_2O_3 ; Óxido de alumínio) em sua forma densa é amplamente utilizada devido à sua biocompatibilidade, inércia química, resistência à oxidação e excelentes propriedades mecânicas. No entanto, essas características bioinertes da alumina densa limitam suas aplicações clínicas pois não permite sítios de ligação direta com os as células e tecidos humanos (GAO et al., 2014). Com o objetivo de melhorar essa característica, diversas técnicas são empregadas, como tratamentos químicos e térmicos (FUJIBAYASHI et al., 2004; TAKEMOTO, 2005). Nos últimos anos pesquisadores observaram que nanofilmes de alumina amorfa nanoporosa apresentam bioatividade, com alta adsorção de proteínas e proliferação de osteoblastos, sendo interessantes para produção de scaffolds com o objetivo de preenchimento de defeitos ósseos (KARLSSON et al., 2003; SONG et al., 2013; POPAT et al., 2007).

Diante disso, este trabalho tem por objetivo caracterização físico-química e avaliação *in vivo* da bioatividade de scaffolds amorfos 3D-nanofibrosos de alumina produzidos pela técnica de SBS (*Solution Blow Spinning*) para regeneração óssea.

2. CAPITULO ÚNICO – ARTIGO

Physicochemical characterization and biological effect of 3d-nanofibrous alumina scaffolds produced by solution blow spinning.

Danyella Carolyna Soares dos Reis¹, Camila Rodrigues Borges Linhares¹, Mariaugusta Ferreira Mota², Deborah Santos Gomes², Gelmires de Araújo Neves², Jonas Dantas Batista³, Paula Dechichi⁴, Leticia de Souza Castro Filice⁵, Romualdo Rodrigues Menezes², Flaviana Soares Rocha⁶

1- Postgraduate Student, Integrated Dental Clinic Program, Faculty of Dentistry, Federal University of Uberlândia, MG, Brazil.

2- Department of Materials Engineering, Federal University of Campina Grande, Campina Grande, PB, Brazil.

3- Department of Oral and Maxillofacial Surgery and Implantology, Federal University of Uberlandia, MG, Brazil.

4- Biomedical Science Institute, Federal University of Uberlândia, MG, Brazil.

5- Faculty of Medicine, Federal University of Uberlândia, MG, Brazil.

6- Dentistry Department, University of Brasília, Brasília, DF, Brazil.

Abstract: Bone substitute biomaterials with the potential to improve cell-material interactions are in high demand. The aim of this study was to perform physicochemical characterization and evaluate *in vivo* the bioactivity of amorphous 3D-nanofibrous alumina scaffolds produced by the SBS (*Solution Blow Spinning*) technique for bone regeneration. The nanofibers used in this study were obtained from a solution of aluminum nitrate, polyvinylpyrrolidone (PVP), ethanol and distilled water, and spun in the SBS apparatus under defined pressure and temperature. The fibers had a macro and microscopic cotton-like 3D structure and were calcined at 500°C. The morphological characterization of the nanofibers was performed using scanning electron microscopy (SEM), and the mineralogical characterization by X-ray diffraction (XRD). To evaluate the biological effect, bone defects were created in the femur of 20 male Wistar rats.

The defects were filled with blood or alumina nanofibers. The animals were euthanized at 14 or 28 days. Femurs were collected and processed to obtain histological slides. Descriptive histological analysis of the bone repair process associated with the biomaterial was performed. Also, bone neoformation and the particles of the remaining graft were quantified for histomorphometry analysis. In the morphological analysis, the nanofibers had a circular cross section with mean diameters of 287 nm; the XRD pattern did not present diffraction reflections, characterizing an amorphous alumina. Histomorphometry revealed a greater amount of bone neoformation in the Alumina groups when compared to the control in the two experimental periods ($p < 0.05$) and the percentage of Alumina graft particles remaining at 14 and 28 days was similar. In conclusion, the tested 3D alumina scaffolds allowed bone deposition and favored bone defect filling with new bone.

Key-words: nanofibrous alumina, three-dimensional scaffold, bone repair.

Introduction

The major challenge of tissue engineering is to design functional materials that can enhance cell-material interactions and improve tissue repair. Various forms of Alumina ceramics have been studied for different applications. Currently, Alumina (Al_2O_3 ; Aluminum oxide) in its dense form is widely used in orthopedic prostheses ¹ and dental implants ² due to their biocompatibility, chemical inertness, resistance to oxidation and excellent mechanical properties ³⁻⁶. However, this bioinert characteristics of dense alumina limits their clinical applications due to the non-active bond with human bone tissue and lack of interaction with the surrounding cells ⁷.

Bone scaffolds with the potential to allow new bone tissue ingrowth are in high demand. In the last years researchers observed that nanoporous amorphous alumina nanofilms (of thin membranes) present bioactivity, with high protein (ex: fibronectin) adsorption, and osteoblast proliferation ^{4,5,8-10}. The first *in vitro* study highlighting the influence of nanometer ceramic grain-size on bone cell adhesion was reported in 1999, demonstrating that osteoblast adhesion was significantly higher on nanophase alumina when compared to micron sized conventional alumina substrates ¹¹.

Few similar studies demonstrated that is possible to influence cellular attachment and mineralization of osteoblasts ^{4,12,13} and mesenchymal stem cells ^{5,14} by varying the pore size of nanostructured amorphous alumina membranes *in vitro*. Most reported studies were made varying anodization processing parameters ^{4,12,14} to produce one-dimensional amorphous nanophase alumina in the form of thin membranes ^{4,5,12-14} with promising results. However, to date, the literature still lacks studies involving the production of three-dimensional (3D) amorphous alumina nanofibrous scaffolds with bioactivity capacity and customized shape to adapt specific damaged bone.

Solution Blow Spinning (SBS) is a simple and rapid nanofiber fabrication technology developed at the beginning of the century ¹⁵. This method produces nanofibers with open fiber networks for enhanced cell infiltration and was efficiently adapted to produce ceramic nanofibers ^{16,17}. Recently, it was demonstrated the potential of SBS for the production of 3D-nanofibrillar scaffolds, as well as nanofibers with nanometric pores ¹⁸. For this reason, the present study aimed to perform physicochemical characterization and assess *in vivo* the bioactivity of amorphous 3D-nanofibrous alumina scaffolds produced by the SBS technique for bone regeneration.

Materials and Methods

Materials:

Aluminum nitrate nonahydrate (Sigma- Aldrich®, Brazil) and polyvinylpyrrolidone (PVP, Mw ~1300000 g/mol, amorphous) were used as inorganic and organic precursors to form hybrid fibers. Ethanol (EtOH, 99.5%, Synth®, Brazil) and distilled water were used as solvents for preparation of the solutions.

Solutions and scaffold production:

Solutions were prepared by dissolving aluminum nitrate nonahydrate (2.206 g) in a 2:1 ethanol/water mixture under vigorous stirring for 1 h. Further, 10wt% of PVP was slowly added to the solution and stirred for 1 h.

The final solution was transferred to a syringe and injected with a rate of 6.6 mL/h into the inner channel of a SBS nozzle. The spinning air pressure was set at 0.34 MPa. Fibers were spun across a tubular furnace with a temperature of 60°C to help solvent evaporation. The fibers were collected on a static collector placed in a chamber at 80°C. The spinning apparatus and processing parameters is detailed in previous works^{16,19,20}. The as-spun fibers formed a 3D cotton-wool-like scaffold (nanostructured in the form of fibers), which were then calcined at 500°C for 2 h.

Physicochemical characterization of the scaffold:

Scaffold morphology was evaluated by scanning electron microscopy (SEM, SSX- 550, Shimadzu, Japan). The fiber diameter was measured using the ImageJ software (National Institute of Health, USA). At least 300 individual fiber diameters were measured. Mineralogical characterization was performed by X-ray diffraction (XRD) (XRD-6000, Shimadzu, Japan) using CuK α radiation ($\lambda=1.5418 \text{ \AA}$) at 40 kV, 30 mA, under fixed time mode with step size of 0.02°.

Animals:

Twenty male Wistar rats (*Rattus norvegicus*) weighing $300 \pm 20\text{g}$ (10 weeks of age) were housed in standard conditions (12-hour light/dark cycle, temperature of $22 \pm 1^\circ\text{C}$ and relative humidity of 50-60%), with food (composition: humidity, crude protein, ethereal extract, mineral, crude fiber, calcium, and phosphorus) and water *ad libitum*. All experimental protocols with animals were approved by the Committee on the Ethics of Animal Use and Care of the Federal University of Uberlândia (permit number 088/17). All procedures were carried out in strict accordance with the recommendations in the Guide for the National Institutes of Health guide for the care and use of Laboratory animals (NIH Publications No. 8023, revised 1978).

Surgical procedure:

After one week of acclimatization, the animals were anaesthetized by an intraperitoneal injection of 100 mg/kg ketamine 10% and 7 mg/kg xylazine 2% hydrochloride. After trichotomy and antisepsis, bone defects were created in both

femurs as described by Batista et al.²¹. Briefly, with the animal positioned in right lateral decubitus, the outer face of the right femur was exposed through a 2cm longitudinal incision. Then, a full-thickness cortical bone osteotomy was made with round bur under saline irrigation, creating a 2.3mm bone defect. The defects were randomly filled with coagulous in the Control Group, and 3D-nanofibrous alumina scaffolds in the Test Group. Then, the defects were distributed into 4 groups (n=5) for each sacrifice period: Control (14 days), Control (28 days), Alumina (14 days) and Alumina (28 days). The wound was closed using Nylon 4.0 suture.

Euthanasia and Sample Collection:

All animals were euthanized 14 or 28 days after surgery by intraperitoneal injection with sodium thiopental and lidocaine, followed by cervical dislocation, in compliance with the principles of the Universal Declaration on Animal Welfare. The diaphysis containing the bone defect were immediately fixed in PBS-buffered formalin (4%) solution (pH 7.4) for 48 hours at room temperature. Subsequently they were washed, the bone was decalcified in 10% ethylene diamine tetra acetic acid fluid (pH7.2) and embedded in paraffin.

Histomorphometry Analysis:

The semi-serial 5 µm sections were obtained from the bone defects center and stained with Hematoxylin and Eosin (HE) and Mallory Trichrome (MT). Histological observations were completed using optical microscopy (Optical Microscope Model Olympus® BX50, Olympus Imaging America Inc. Shinjuku-ku, Tokyo / Japan).

The percentage of the newly formed bone and remnant graft particles by the total area of the bone defect was determined using 3 Mallory Trichrome stained sections for each defect, as described by Batista et al. (2014). Briefly, the bone defect (region of interest - ROI) was delimited with four straight lines from the edges of the injured cortical to the opposite cortical. The percentage of newly formed bone/remnant graft particles within this area was quantified with the

measuring tool of Image J 1.53 (Wayne Rasband, National Institutes of Health, EUA).

Statistical Analysis

Data were analyzed using GraphPad Prism (GraphPad Prism® version 5.0 for Windows, San Diego, CA, USA). Initially, the values obtained were submitted to the Kolmogorov-Smirnov normality test. The parameters were analyzed using unpaired t-tests and the differences were considered statistically significant if $p < 0.05$.

Results

Scaffold characterization:

Nanofibers with an approximately circular cross section were produced. Small number of bead-shaped structures was observed (Figure 1A-B). This is attributed to instabilities in the spinning process, and was also observed in other works on SBS of oxide ceramic nanofibers^{16,20}. The fiber diameter distribution is shown in Figure 1C. The fibers presented an average diameter of 287nm and a broad diameter distribution, with majority of fibers in the range of 100 to 500nm.

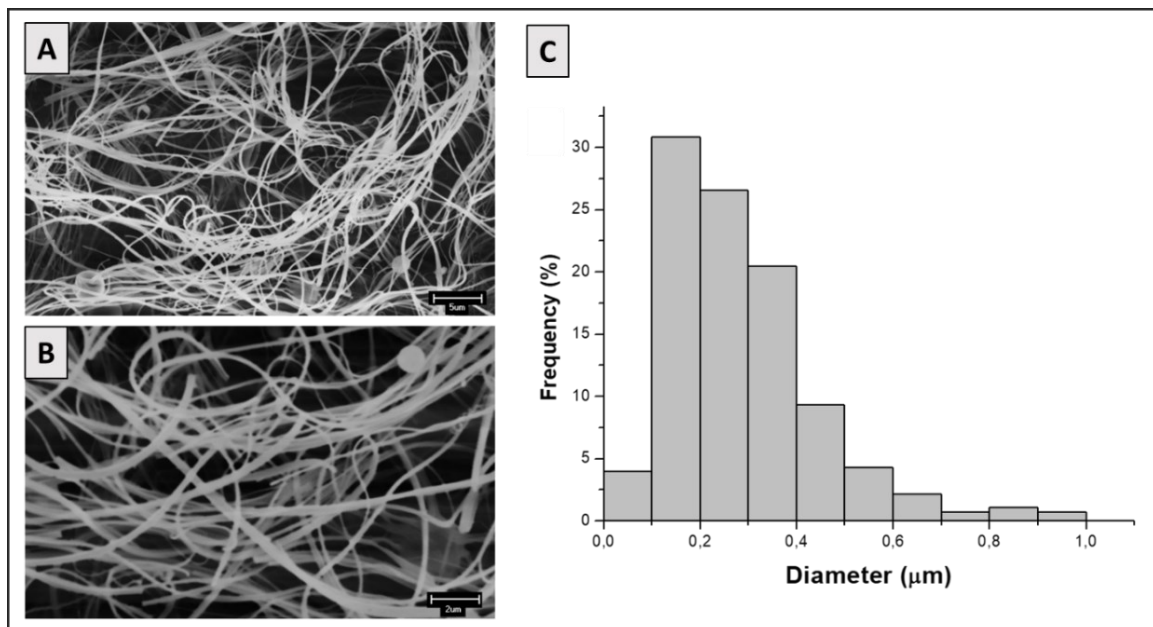


Figure 1: (A-B) Scanning Electron Microscope (SEM) images in different magnification; (C) Graphical distribution of the fiber diameter of the produced 3D-nanofibrous alumina scaffolds. (Magnification indicated in the image).

The XRD pattern of the produced 3D-nanofibrillar alumina scaffolds is shown in Figure 2. The pattern did not present diffraction reflections, which is characteristic of an amorphous material.

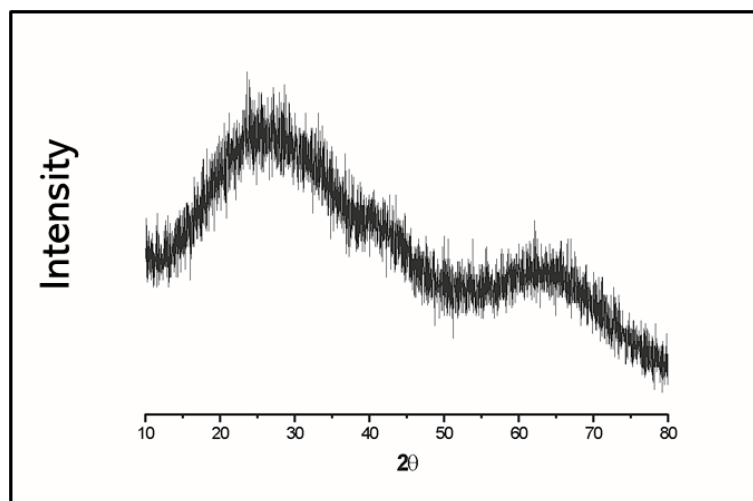


Figure 2: XRD patterns of the produced 3D-nanofibrous alumina scaffolds.

Biological effect - Histological observations and histomorphometry analysis:

In Control Group, the areas presented bone tissue with normal morphological appearance, forming trabeculae that delimited small cavities filling partially the defect. In Alumina Group, primary bone tissue was predominant in the defect, with large number of osteocytes included in the bone matrix, associated with numerous remnant particles of the graft. Areas of secondary bone tissue were infrequent, even after 28 days. Cubic osteoblasts with marked cytoplasmic basophilia were observed lining the bone matrix, indicating intense activity of protein synthesis. Remnant graft particles incorporated into the bone matrix, with signs of remodeling were frequently seen (Figure 3).

Histomorphometry revealed higher amount of newly formed bone in Alumina groups when compared to Control in both experimental periods ($p < 0.05$).

The percentage of remnant graft in Alumina group at 14 and 28 days was similar (Figure 4).

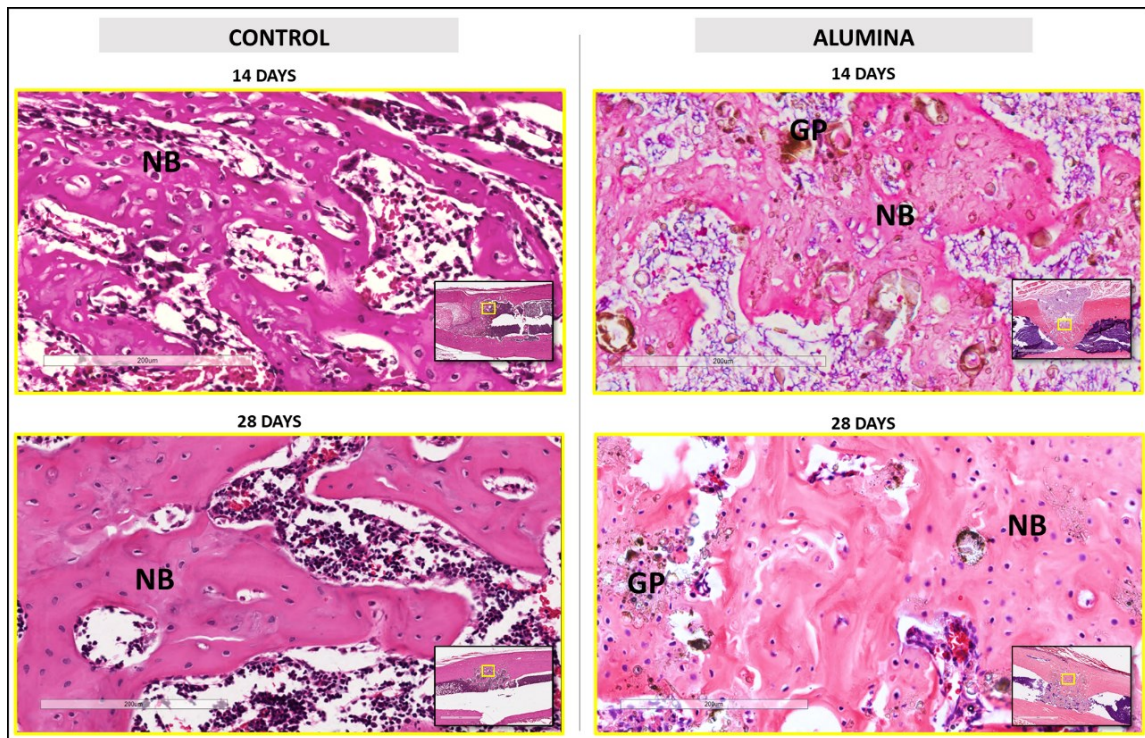


Figure 3: New bone formation in Control and Alumina Groups. Note the new bone formation associated with the remnant graft particles in Alumina. NB: new bone; GP: graft particles. HE (Magnification indicated in the image).

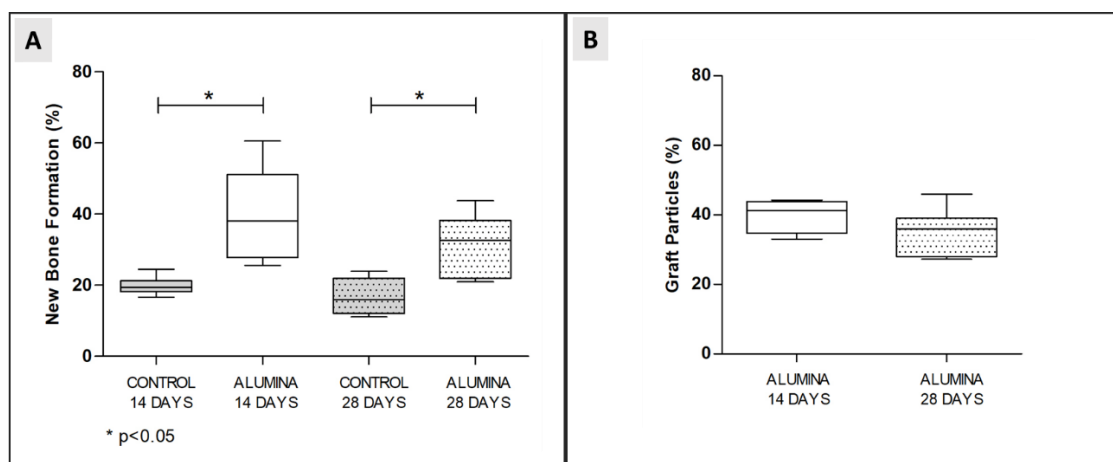


Figure 4: Histomorphometry analysis of New Bone Formation (A) and Graft Particles (B) in Control and Alumina Groups after 14- and 28-days implantation (*p<0.05).

Discussion

The present study is the first using the innovative amorphous 3D-nanofibrous alumina scaffolds (nanostructured in the form of fibers) obtained using thermal treatment of SBS aiming to achieve appropriate open structure for bone regeneration. The proposed technique differs from those usually found in the literature for the production of alumina-based biomaterials.

The nanostructured alumina materials are usually prepared with anodization processing ^{4,12,14}. Although promising, this method offers limitations for 3D-scaffold production in the form of fibers at nanoscale. Anodized alumina, for example, is produced from aluminum, which has a limit on the total volume that can be anodized. This is why most studies using this method evaluated nanostructured alumina in the form of membranes with reduced thickness ^{4,5,12-14}. On the other hand, electrospinning (ES) is the most used top-down method for the production of ceramic nanofibers ²²⁻²⁴. Studies using this method reported the production of: (1) alpha alumina (α -Al₂O₃) fibers with diameters from 20 to 500 nm after 900 to 1300°C calcination ²⁵; (2) α -Al₂O₃ fibers with diameters from 150 to 500 nm after calcining at 1200°C ²²; (3) α -Al₂O₃ fibers with diameters from 100 to 500nm after firing at 1000°C ²³; and (4) α -Al₂O₃ fibers with diameters from 102 to 378nm after firing at 1200°C ²⁴. ES for the production of γ -phase alumina (γ -Al₂O₃) fibers with diameters from 114 to 390nm after calcining at 800°C was also reported ²⁴. However, it is important to note that ES is time-consuming, and fibers are not easily assembled into large-scale 3D structures leading to unsuitable porous structure ²⁶.

Compared to the above mentioned methods, SBS is interesting because the morphological properties of the produced scaffolds are more selectively designed ^{15,18} to meet the specificity of bone repair needs. It also allows control of material properties, such as pore size and membrane thickness, in a reproducible manner ^{15,26}. The fibers are rapidly processed and collected into

different architectures such as cotton-wool-like structures. Because of this, SBS can potentially be used to generate 3D-nano scaffolds in the form of fibers with high porosity at nanometric scale ^{16,17}. Therefore, SBS presents a high-yielding and is one of most promising technique for development of 3D-nanofibrous systems.

Recently, some studies produced amorphous γ -Al₂O₃ and α -Al₂O₃ nano and microfibers using SBS ^{27,28} with mean diameters of 4 μ m (varying from 3.0 μ m to 5.5 μ m) ²⁷ and in the range of 1.5 up to 47 ²⁸. However, these studies did not observe fiber diameter and 3D cotton-like structures such those achieved in the present work. That is why the 3D-architecture and nanofibrous characteristics of the material produced by our study is innovate and permit its use in several potential application.

The clinical success of new ceramic materials lies on the events that happen largely at the tissue-material interface ²⁹. Once the graft is placed in a bone defect, the regions within distinct particles are engulfed by a blood clot. This clot supplies the necessary proteins/growth factors needed to begin the cell adhesion process and ultimately the repair of bone ²⁹. Thus, given that biomaterial surfaces are the first to interact with the host, such surface characteristics, degree of porosity ³⁰⁻³² and material chemistry ^{30,32} are of the utmost importance concerning the subsequent biological cascade leading to bone healing. Ideally, a bioactive graft material would interact with surrounding cells and allow for the formation of bone together with safe biodegradation ⁷. Considering this, the unique features of nanofibrous alumina offer promising possibilities for different approaches in tissue engineering (Mussano et al., 2018).

In the present study, 3D-nanofibrous alumina scaffolds were used in an animal model to assess bone regeneration. The results demonstrated greater bone neoformation for alumina groups when compared to the control, with a rate of biomaterial degradation similar to the rate of bone formation. This is especially important for bone substitutes because the resorption of the biomaterial cannot be faster than bone deposition, allowing the defect to be filled with new bone and maintain its original architecture ⁷. It was possible to verify the progress of bone

remodeling in control and experimental groups demonstrating that the tested scaffolds were biocompatible and bioactive, presenting osteoinductive and osteoconductive activity.

These favorable events observed *in vivo* are greatly influenced by the material porosity³⁰⁻³² and chemistry^{30,32}, and involves recruitment and penetration of cells from the surrounding bone tissue, as well as vascularization. The penetration of vessels is possible, in part, due to the porosity of the material. This is an important issue for oxygen supply, nutrients transport and waste exist from the cells responsible for bone repair⁶. It is also well established in the literature that pore size and porosity of scaffolds mediate the response of mesenchymal cells^{5,33}, increasing long-term osteogenic differentiation and proliferation^{4,12}, being mandatory for the clinical success of biomaterial. Although specific bone cell behavior was not evaluated *in vitro*, in the present *in vivo* study the 3D-alumina scaffolds with pores ranging from 100 to 500nm were successfully used for bone repair and regeneration.

The interaction between the cells and surface of the amorphous 3D-nanofibrous alumina scaffolds can also be the result of its hydrophilicity. It has been reported that nanophase alumina is more hydrophilic than conventional alumina¹¹. This may influence on cell adhesion^{6,33} and favor the observed bone deposition. In fact, better adhesion of hFOB1.19 human osteoblasts are found on the more hydrophilic materials that presented a higher protein adsorption³⁴. As a consequence, right after scaffold implantation, essential interaction of proteins with the biomaterial surfaces occurs³⁵ creating a stable and highly topographically complex surface at the nanoscale in which bone deposition can occur.

The amorphous or crystalline phases of ceramic scaffolds can influence the osteogenic induction process³⁰. Nanostructured amorphous alumina membranes already demonstrated osteoinductive potential after *in vitro* studies⁴. These results depicted the produced nanofibers can present similar responses *in vivo*, despite the differences in spinning techniques and material structure. The alumina used in the present experiment, was calcined at 500°C to produce

amorphous 3D-nanofibrous alumina scaffolds as confirmed during fiber characterization. Degradation of amorphous materials occurs faster than crystalline ones due to the disordered nature of its molecular chains which lead to less density of the material ⁶. Even so, the reabsorption speed of the tested 3D-alumina scaffolds allowed bone deposition and favored the bone defect to be adequately filled with new bone.

Acknowledgements: The authors would like to thank CNPq (grant nos. 308822/2018-8 and 420004/2018-1), FAPEMIG (grant no. 03063-16) and FAPESQ (Bidding Term Pronex 001/2019) for the financial support. Authors thank D.Sc. Rosiane Maria da Costa Farias for the support in the spinning process.

Conflict of interest: The authors declare no conflict of interest.

References

1. Hannouche D, Zaoui A, Zadegan F, et al. Thirty years of experience with alumina-on-alumina bearings in total hip arthroplasty. *Int Orthop* 2011; 35: 207–213. DOI: [10.1007/s00264-010-1187-1](https://doi.org/10.1007/s00264-010-1187-1).
2. Schierano G, Mussano F, Faga MG, et al. An alumina toughened zirconia composite for dental implant application: In vivo animal results. *Biomed Res Int*; 2015. Epub ahead of print 2015. DOI: [10.1155/2015/157360](https://doi.org/10.1155/2015/157360).
3. Piconi C, Porporati AA. Bioinert ceramics: Zirconia and alumina. In: *Handbook of Bioceramics and Biocomposites*. 2016, pp. 59–89. DOI: [10.1007/978-3-319-12460-5_4](https://doi.org/10.1007/978-3-319-12460-5_4)
4. Karlsson M, Pålsgård E, Wilshaw PR, et al. Initial in vitro interaction of osteoblasts with nano-porous alumina. *Biomaterials* 2003; 24: 3039–3046. DOI: [10.1016 / s0142-9612 \(03\) 00146-7](https://doi.org/10.1016/s0142-9612(03)00146-7).
5. Song Y, Ju Y, Song G, et al. In vitro proliferation and osteogenic differentiation of mesenchymal stem cells on nanoporous alumina. *Int J Nanomedicine* 2013; 8: 2745–2756. DOI: [10.2147 / IJN.S44885](https://doi.org/10.2147 / IJN.S44885).
6. Toloue EB, Karbasi S, Salehi H, et al. Potential of an electrospun composite scaffold of poly (3-hydroxybutyrate)-chitosan/alumina nanowires in bone tissue engineering applications. *Mater Sci Eng C* 2019; 99: 1075–1091.

- DOI: [10.1016/j.msec.2019.02.062](https://doi.org/10.1016/j.msec.2019.02.062).
7. Gao C, Deng Y, Feng P, et al. Current progress in bioactive ceramic scaffolds for bone repair and regeneration. *Int J Mol Sci* 2014; 15: 4714–4732. DOI: [10.3390 / ijms15034714](https://doi.org/10.3390/ijms15034714).
 8. Popat KC, Leary Swan EE, Mukhatyar V, et al. Influence of nanoporous alumina membranes on long-term osteoblast response. *Biomaterials* 2005; 26: 4516–4522. DOI: [10.1016 / j.biomaterials.2004.11.026](https://doi.org/10.1016 / j.biomaterials.2004.11.026).
 9. Naji A, Harmand MF. Cytocompatibility of two coating materials, amorphous alumina and silicon carbide, using human differentiated cell cultures. *Biomaterials* 1991; 12: 690–694. DOI: [10.1016 / 0142-9612 \(91\) 90118-t](https://doi.org/10.1016 / 0142-9612 (91) 90118-t).
 10. Leary Swan EE, Popat KC, Desai TA. Peptide-immobilized nanoporous alumina membranes for enhanced osteoblast adhesion. *Biomaterials* 2005; 26: 1969–1976. DOI: [10.1016 / j.biomaterials.2004.07.001](https://doi.org/10.1016 / j.biomaterials.2004.07.001).
 11. Webster TJ, Siegel RW, Bizios R. Osteoblast adhesion on nanophase ceramics. *Biomaterials* 1999; 20: 1221–1227. DOI: [10.1016 / s0142-9612 \(99\) 00020-4](https://doi.org/10.1016 / s0142-9612 (99) 00020-4).
 12. Mussano F, Genova T, Serra FG, et al. Nano-pore size of alumina affects osteoblastic response. *Int J Mol Sci* 2018; 19: 1–12. DOI: [10.3390 / ijms19020528](https://doi.org/10.3390 / ijms19020528).
 13. Song Y, Ju Y, Morita Y, et al. Effect of the nanostructure of porous alumina on growth behavior of MG63 osteoblast-like cells. *J Biosci Bioeng* 2013; 116: 509–515. DOI: [10.1016 / j.jbiosc.2013.04.007](https://doi.org/10.1016 / j.jbiosc.2013.04.007).
 14. Popat KC, Chalvanichkul KI, Barnes GL, et al. Osteogenic differentiation of marrow stromal cells cultured on nanoporous alumina surfaces. *J Biomed Mater Res - Part A* 2007; 80: 955–964. DOI: [10.1002 / jbm.a.31028](https://doi.org/10.1002 / jbm.a.31028).
 15. Medeiros ES, Glenn GM, Klamczynski AP, et al. Solution blow spinning: A new method to produce micro- and nanofibers from polymer solutions. *J Appl Polym Sci* 2009; 113: 2322–2330. DOI: [10.1002/app.30275](https://doi.org/10.1002/app.30275).
 16. Costa DL, Leite RS, Neves GA, et al. Synthesis of TiO₂ and ZnO nano and submicrometric fibers by solution blow spinning. *Mater Lett* 2016; 183: 109–113. DOI: [10.1016 / j.matlet.2016.07.073](https://doi.org/10.1016 / j.matlet.2016.07.073).

17. Santos AMC, Mota MF, Leite RS, et al. Solution blow spun titania nanofibers from solutions of high inorganic/organic precursor ratio. *Ceram Int* 2018; 44: 1681–1689. DOI: [10.1016 / j.ceramint.2017.10.096](https://doi.org/10.1016/j.ceramint.2017.10.096).
18. Medeiros ELG, Gomes DS, Santos AMC, et al. 3D nanofibrous bioactive glass scaffolds produced by one-step spinning process. *Ceram Int* 2021; 47: 102–110. DOI: [10.1016/j.ceramint.2020.08.112](https://doi.org/10.1016/j.ceramint.2020.08.112).
19. da Costa Farias RM, Severo LL, da Costa DL, et al. Solution blow spun spinel ferrite and highly porous silica nanofibers. *Ceram Int* 2018; 44: 10984–10989. DOI: [10.1016 / j.ceramint.2018.03.099](https://doi.org/10.1016/j.ceramint.2018.03.099).
20. Farias RMDC, Menezes RR, Oliveira JE, et al. Production of submicrometric fibers of mullite by solution blow spinning (SBS). *Mater Lett* 2015; 149: 47–49. DOI: [10.1016 / j.matlet.2015.02.111](https://doi.org/10.1016/j.matlet.2015.02.111)
21. Batista JD, Zanetta-Barbosa D, Cardoso S V., et al. Effect of low-level laser therapy on repair of the bone compromised by radiotherapy. *Lasers Med Sci* 2014; 29: 1913–1918. DOI: [10.1007 / s10103-014-1602-8](https://doi.org/10.1007/s10103-014-1602-8).
22. Yu H, Guo J, Zhu S, et al. Preparation of continuous alumina nanofibers via electrospinning of PAN/DMF solution. *Mater Lett* 2012; 74: 247–249. DOI: [10.1016/j.matlet.2012.01.077](https://doi.org/10.1016/j.matlet.2012.01.077).
23. Mahapatra A, Mishra BG, Hota G. Studies on electrospun alumina nanofibers for the removal of chromium(vi) and fluoride toxic ions from an aqueous system. *Ind Eng Chem Res* 2013; 52: 1554–1561. DOI: [10.1021/ie301586j](https://doi.org/10.1021/ie301586j)
24. Kim JH, Yoo SJ, Kwak DH, et al. Characterization and application of electrospun alumina nanofibers. *Nanoscale Res Lett* 2014; 9: 1–6. DOI: [10.1186 / 1556-276X-9-44](https://doi.org/10.1186/1556-276X-9-44).
25. Panda PK, Ramakrishna S. Electrospinning of alumina nanofibers using different precursors. *J Mater Sci* 2007; 42: 2189–2193. DOI: [10.1007/s10853-007-1581-2](https://doi.org/10.1007/s10853-007-1581-2).
26. Medeiros ELG, Braz AL, Porto IJ, et al. Porous Bioactive Nanofibers via Cryogenic Solution Blow Spinning and Their Formation into 3D Macroporous Scaffolds. *ACS Biomater Sci Eng* 2016; 2: 1442–1449. DOI: [10.1021 / acsbiomaterials.6b00072](https://doi.org/10.1021/acsbiomaterials.6b00072).

27. Li L, Kang W, Zhuang X, et al. A comparative study of alumina fibers prepared by electro-blown spinning (EBS) and solution blowing spinning (SBS). *Mater Lett* 2015; 160: 533–536. DOI: [10.1016 / j.matlet.2015.08.016](https://doi.org/10.1016/j.matlet.2015.08.016).
28. Li L, Kang W, Zhao Y, et al. Preparation of flexible ultra-fine Al₂O₃ fiber mats via the solution blowing method. *Ceram Int* 2015; 41: 409–415. DOI: [10.1016/j.ceramint.2014.08.085](https://doi.org/10.1016/j.ceramint.2014.08.085).
29. Masters KS, Anseth KS. Cell-Material Interactions. *Adv Chem Eng* 2004; 29: 7–46. DOI: [10.1016/S0065-2377\(03\)29002-5](https://doi.org/10.1016/S0065-2377(03)29002-5).
30. Price RL, Gutwein LG, Kaledin L, et al. Osteoblast function on nanophase alumina materials: Influence of chemistry, phase, and topography. *J Biomed Mater Res - Part A* 2003; 67: 1284–1293. DOI: [10.1002 / jbm.a.20011](https://doi.org/10.1002/jbm.a.20011)
31. Tran N, Webster TJ. Nanotechnology for bone materials. *Wiley Interdiscip Rev Nanomedicine Nanobiotechnology* 2009; 1: 336–351. DOI: [10.1002 / wnan.23](https://doi.org/10.1002/wnan.23).
32. Hing KA. Bioceramic bone graft substitutes: Influence of porosity and chemistry. *Int J Appl Ceram Technol* 2005; 2: 184–199. DOI: [10.1111/j.1744-7402.2005.02020.x](https://doi.org/10.1111/j.1744-7402.2005.02020.x).
33. Ni S, Li C, Ni S, et al. Understanding improved osteoblast behavior on select nanoporous anodic alumina. *Int J Nanomedicine* 2014; 9: 3325–3334. DOI: [10.2147/IJN.S60346](https://doi.org/10.2147/IJN.S60346).
34. Liu X, Lim JY, Donahue HJ, et al. Influence of substratum surface chemistry/energy and topography on the human fetal osteoblastic cell line hFOB 1.19: Phenotypic and genotypic responses observed in vitro. *Biomaterials* 2007; 28: 4535–4550. DOI: [10.1016/j.biomaterials.2007.06.016](https://doi.org/10.1016/j.biomaterials.2007.06.016).
35. Anselme K, Ponche A, Biggerelle M. Relative influence of surface topography and surface chemistry on cell response to bone implant materials. Part 2: Biological aspects. *Proc Inst Mech Eng Part H J Eng Med* 2010; 224: 1487–1507. DOI: [10.1243/09544119JEIM901](https://doi.org/10.1243/09544119JEIM901).

3. CONCLUSÃO

A técnica de fiação por sopro em solução foi eficiente para obtenção de scaffolds nanofibrilares tridimensionais de alumina com capacidade de otimizar o preenchimento de defeitos ósseos.

REFERÊNCIAS BIBLIOGRÁFICAS

1. Melville JC, NassaRI NN, Hanna IA, Shum JW, Wong ME, Young S. Immediate Transoral Allogeneic Bone Grafting for Large Mandibular Defects. Less Morbidity, More Bone. A Paradigm in Benign Tumor Mandibular Reconstruction? **J Oral Maxillofac Surg**. 2016: S0278-2391(16)30911-9. DOI: [10.1016/j.joms.2016.09.049](https://doi.org/10.1016/j.joms.2016.09.049)
2. Conway JD. Autograft and nonunions: Morbidity with intramedullary bone graft versus iliac crest bone graft. **Orthop Clin North Am**. 2010;41:75–84. DOI: [10.1016/j.ocl.2009.07.006](https://doi.org/10.1016/j.ocl.2009.07.006).
3. Guastaldi, AC. Biomaterial - ponderações sobre as publicações científicas. **Rev. APCD**. 2004.
4. Boss JH, Shajrawi I, Aunullah J, Mendes DG. The relativity of biocompatibility. A critique of the concept of biocompatibility. **Isr J Med Sci**. 1995 Apr;31(4):203-9.
5. Hejazi F, Mirzadeh H. Roll-designed 3D nanofibrous scaffold suitable for the regeneration of load bearing bone defects. **Prog Biomater**. 2016;5(3-4):199-211. DOI: [10.1007/s40204-016-0058-2](https://doi.org/10.1007/s40204-016-0058-2).
6. Karageorgiou V, Kaplan D. Porosity of 3D biomaterial scaffolds and osteogenesis. **Biomaterials**. 2005; 26(27):5474-5491. DOI: [10.1016/j.biomaterials.2005.02.002](https://doi.org/10.1016/j.biomaterials.2005.02.002).
7. Gao C, et al. Current progress in bioactive ceramic scaffolds for bone repair and regeneration. **Int J Mol Sci**. 2014; 15(3): 4714–4732. DOI: [10.3390/ijms15034714](https://doi.org/10.3390/ijms15034714).
8. Vallet-Regí M. Nanostructured mesoporous silica matrices in nanomedicine. **Journal of Internal Medicine**. 2010; 267(1):22-43. DOI: [10.1111/j.1365-2796.2009.02190.x](https://doi.org/10.1111/j.1365-2796.2009.02190.x).
9. Jun-Hyeog J, et al. Electrospun materials as potential platforms for bone tissue engineering. **Adv. Drug Deliv. Rev**. 2009; 61: 1065–1083. DOI: [10.1016/j.addr.2009.07.008](https://doi.org/10.1016/j.addr.2009.07.008).

10. Medeiros ES, et al. Solution Blow Spinning: A New Method to Produce Micro- and Nanofibers from Polymer Solutions. **J Appl Polym Sci.** 2009; 113(4):2322-2330. DOI:[10.1002/app.30275](https://doi.org/10.1002/app.30275).
11. Bonan RF, et al. In vitro antimicrobial activity of solution blow spun poly(lactic acid)/polyvinylpyrrolidone nanofibers loaded with Copaiba (Copaifera sp.) oil. **Mat Sci Eng C-Mater.** 2015; 48:372-377. DOI: [10.1016/j.msec.2014.12.021](https://doi.org/10.1016/j.msec.2014.12.021).
12. Fujibayashi S, et al. Osteoinduction of porous bioactive titanium metal. **Biomaterials.** 2004; 25(3):443-450. DOI:[10.1016/S0142-9612\(03\)00551-9](https://doi.org/10.1016/S0142-9612(03)00551-9).
13. Takemoto M. Mechanical properties and osteoconductivity of porous bioactive titanium. **Biomaterials.** 2005; 26(30):6014-23. DOI: [10.1016/j.biomaterials.2005.03.019](https://doi.org/10.1016/j.biomaterials.2005.03.019)
14. Hannouche D, Zaoui A, Zadegan F, et al. Thirty years of experience with alumina-on-alumina bearings in total hip arthroplasty. **Int Orthop** 2011; 35: 207–213. DOI: [10.1007/s00264-010-1187-1](https://doi.org/10.1007/s00264-010-1187-1).
15. Schierano G, Mussano F, Faga MG, et al. An alumina toughened zirconia composite for dental implant application: In vivo animal results. **Biomed Res Int.** 2015. DOI: [10.1155/2015/157360](https://doi.org/10.1155/2015/157360).
16. Piconi C, Porporati AA. Bioinert ceramics: Zirconia and alumina. In: Handbook of Bioceramics and Biocomposites. 2016, pp. 59–89. DOI: [10.1007/978-3-319-12460-5_4](https://doi.org/10.1007/978-3-319-12460-5_4).
17. Karlsson M, Pålsgård E, Wilshaw PR, et al. Initial in vitro interaction of osteoblasts with nano-porous alumina. **Biomaterials.** 2003; 24: 3039–3046. DOI: [10.1016 / s0142-9612 \(03\) 00146-7](https://doi.org/10.1016 / s0142-9612 (03) 00146-7)

18. Song Y, Ju Y, Song G, et al. In vitro proliferation and osteogenic differentiation of mesenchymal stem cells on nanoporous alumina. **Int J Nanomedicine**. 2013; 8: 2745–2756. DOI: [10.2147 / IJN.S44885](https://doi.org/10.2147/IJN.S44885).
19. Toloue EB, Karbasi S, Salehi H, et al. Potential of an electrospun composite scaffold of poly (3-hydroxybutyrate)-chitosan/alumina nanowires in bone tissue engineering applications. **Mater Sci Eng C**. 2019; 99: 1075–1091. DOI:[10.1016/j.msec.2019.02.062](https://doi.org/10.1016/j.msec.2019.02.062).
20. Popat KC, Leary Swan EE, Mukhatyar V, et al. Influence of nanoporous alumina membranes on long-term osteoblast response. **Biomaterials**. 2005; 26: 4516–4522. DOI: [10.1016/j.biomaterials.2004.11.026](https://doi.org/10.1016/j.biomaterials.2004.11.026).
21. Naji A, Harmand MF. Cytocompatibility of two coating materials, amorphous alumina and silicon carbide, using human differentiated cell cultures. **Biomaterials**. 1991; 12: 690–694. DOI: [10.1016/0142-9612\(91\)90118-t](https://doi.org/10.1016/0142-9612(91)90118-t).
22. Leary Swan EE, Popat KC, Desai TA. Peptide-immobilized nanoporous alumina membranes for enhanced osteoblast adhesion. **Biomaterials**. 2005; 26: 1969–1976. DOI: [10.1016/j.biomaterials.2004.07.001](https://doi.org/10.1016/j.biomaterials.2004.07.001).
23. Webster TJ, Siegel RW, Bizios R. Osteoblast adhesion on nanophase ceramics. **Biomaterials**. 1999; 20: 1221–1227. DOI: [10.1016/s0142-9612\(99\)00020-4](https://doi.org/10.1016/s0142-9612(99)00020-4).
24. Mussano F, Genova T, Serra FG, et al. Nano-pore size of alumina affects osteoblastic response. **Int J Mol Sci**. 2018; 19: 1–12. DOI: [10.3390/ijms19020528](https://doi.org/10.3390/ijms19020528).
25. Song Y, Ju Y, Morita Y, et al. Effect of the nanostructure of porous alumina on growth behavior of MG63 osteoblast-like cells. **J Biosci Bioeng**. 2013; 116: 509–515. DOI: [10.1016/j.jbiosc.2013.04.007](https://doi.org/10.1016/j.jbiosc.2013.04.007).
26. Popat KC, Chalvanichkul KI, Barnes GL, et al. Osteogenic differentiation of marrow stromal cells cultured on nanoporous alumina surfaces. **J Biomed Mater Res - Part A**. 2007; 80: 955–964. DOI: [10.1002/jbm.a.31028](https://doi.org/10.1002/jbm.a.31028).

27. Costa DL, Leite RS, Neves GA, et al. Synthesis of TiO₂ and ZnO nano and submicrometric fibers by solution blow spinning. **Mater Lett.** 2016; 183: 109–113. DOI:[10.1016/j.matlet.2016.07.073](https://doi.org/10.1016/j.matlet.2016.07.073).
28. Santos AMC, Mota MF, Leite RS, et al. Solution blow spun titania nanofibers from solutions of high inorganic/organic precursor ratio. **Ceram Int.** 2018; 44: 1681–1689. DOI:[10.1016/j.ceramint.2017.10.096](https://doi.org/10.1016/j.ceramint.2017.10.096).
29. Medeiros ELG, Gomes DS, Santos AMC, et al. 3D nanofibrous bioactive glass scaffolds produced by one-step spinning process. **Ceram Int.** 2021; 47: 102–110. DOI: [10.1016/j.ceramint.2020.08.112](https://doi.org/10.1016/j.ceramint.2020.08.112).
30. da Costa Farias RM, Severo LL, da Costa DL, et al. Solution blow spun spinel ferrite and highly porous silica nanofibers. **Ceram Int.** 2018; 44: 10984–10989. DOI:[10.1016/j.ceramint.2018.03.099](https://doi.org/10.1016/j.ceramint.2018.03.099).
31. Farias RMDC, Menezes RR, Oliveira JE, et al. Production of submicrometric fibers of mullite by solution blow spinning (SBS). **Mater Lett.** 2015; 149: 47–49. DOI:[10.1016/j.matlet.2015.02.111](https://doi.org/10.1016/j.matlet.2015.02.111).
32. Batista JD, Zanetta-Barbosa D, Cardoso S V., et al. Effect of low-level laser therapy on repair of the bone compromised by radiotherapy. **Lasers Med Sci.** 2014; 29: 1913–1918. DOI: [10.1007/s10103-014-1602-8](https://doi.org/10.1007/s10103-014-1602-8).
33. Yu H, Guo J, Zhu S, et al. Preparation of continuous alumina nanofibers via electrospinning of PAN/DMF solution. **Mater Lett.** 2012; 74: 247–249. DOI: [10.1016/j.matlet.2012.01.077](https://doi.org/10.1016/j.matlet.2012.01.077).
34. Mahapatra A, Mishra BG, Hota G. Studies on electrospun alumina nanofibers for the removal of chromium(vi) and fluoride toxic ions from an aqueous system. **Ind Eng Chem Res.** 2013; 52: 1554–1561. DOI: [10.1021/ie301586j](https://doi.org/10.1021/ie301586j).
35. Kim JH, Yoo SJ, Kwak DH, et al. Characterization and application of electrospun alumina nanofibers. **Nanoscale Res Lett.** 2014; 9: 1–6. DOI: [10.1186/1556-276X-9-44](https://doi.org/10.1186/1556-276X-9-44).

36. Panda PK, Ramakrishna S. Electrospinning of alumina nanofibers using different precursors. **J Mater Sci.** 2007; 42: 2189–2193. DOI: [10.1007/s10853-007-1581-2](https://doi.org/10.1007/s10853-007-1581-2).
37. Medeiros ELG, Braz AL, Porto IJ, et al. Porous Bioactive Nanofibers via Cryogenic Solution Blow Spinning and Their Formation into 3D Macroporous Scaffolds. **ACS Biomater Sci Eng.** 2016; 2: 1442–1449. DOI: [10.1021/ACSBIMATERIALS.6B00072](https://doi.org/10.1021/ACSBIMATERIALS.6B00072).
38. Li L, Kang W, Zhuang X, et al. A comparative study of alumina fibers prepared by electro-blown spinning (EBS) and solution blowing spinning (SBS). **Mater Lett.** 2015; 160: 533–536. DOI: [10.1016/j.matlet.2015.08.016](https://doi.org/10.1016/j.matlet.2015.08.016).
39. Li L, Kang W, Zhao Y, et al. Preparation of flexible ultra-fine Al₂O₃ fiber mats via the solution blowing method. **Ceram Int.** 2015; 41: 409–415 DOI: [10.1016/j.ceramint.2014.08.085](https://doi.org/10.1016/j.ceramint.2014.08.085).
40. Masters KS, Anseth KS. Cell-Material Interactions. **Adv Chem Eng.** 2004; 29: 7–46 DOI: [10.1016/S0065-2377\(03\)29002-5](https://doi.org/10.1016/S0065-2377(03)29002-5).
41. Price RL, Gutwein LG, Kaledin L, et al. Osteoblast function on nanophase alumina materials: Influence of chemistry, phase, and topography. **J Biomed Mater Res - Part A.** 2003; 67: 1284–1293. DOI: [10.1002/jbm.a.20011](https://doi.org/10.1002/jbm.a.20011).
42. Tran N, Webster TJ. Nanotechnology for bone materials. **Wiley Interdiscip Rev Nanomedicine Nanobiotechnology.** 2009; 1: 336–351. DOI: [10.1002/wnan.23](https://doi.org/10.1002/wnan.23).
43. Hing KA. Bioceramic bone graft substitutes: Influence of porosity and chemistry. **Int J Appl Ceram Technol.** 2005; 2: 184–199. DOI: [10.1111/j.1744-7402.2005.02020.x](https://doi.org/10.1111/j.1744-7402.2005.02020.x).
44. Ni S, Li C, Ni S, et al. Understanding improved osteoblast behavior on select nanoporous anodic alumina. **Int J Nanomedicine.** 2014; 9: 3325–3334. DOI: [10.2147/IJN.S60346](https://doi.org/10.2147/IJN.S60346).

45. Liu X, Lim JY, Donahue HJ, et al. Influence of substratum surface chemistry/energy and topography on the human fetal osteoblastic cell line hFOB 1.19: Phenotypic and genotypic responses observed in vitro. **Biomaterials.** 2007; 28: 4535–4550. DOI:[10.1016/j.biomaterials.2007.06.016](https://doi.org/10.1016/j.biomaterials.2007.06.016).
46. Anselme K, Ponche A, Bigerelle M. Relative influence of surface topography and surface chemistry on cell response to bone implant materials. Part 2: Biological aspects. **Proc Inst Mech Eng Part H J Eng Med.** 2010; 224: 1487–1507. DOI:[10.1243/09544119JEIM901](https://doi.org/10.1243/09544119JEIM901).

ANEXO 1



Universidade Federal de Uberlândia

– Comissão de Ética na Utilização de Animais –



CERTIFICADO

Certificamos que o projeto intitulado "Avaliação Do Potencial Osteocondutor De Nanofibras Enriquecidas Com Diferentes Materiais: Estudo In Vivo", protocolo nº 088/17, sob a responsabilidade de **Jonas Dantas Batista** – que envolve a produção, manutenção e/ou utilização de animais pertencentes ao filo Chordata, subfilo Vertebrata, para fins de pesquisa científica – encontra-se de acordo com os preceitos da Lei nº 11.794, de 8 de outubro de 2008, do Decreto nº 6.899, de 15 de julho de 2009, e com as normas editadas pelo Conselho Nacional de Controle da Experimentação Animal (CONCEA), e foi **APROVADA** pela COMISSÃO DE ÉTICA NA UTILIZAÇÃO DE ANIMAIS (CEUA) da UNIVERSIDADE FEDERAL DE UBERLÂNDIA, em reunião **23 de Fevereiro de 2018**.

(We certify that the project entitled "Avaliação Do Potencial Osteocondutor De Nanofibras Enriquecidas Com Diferentes Materiais: Estudo In Vivo", protocol 088/17, under the responsibility of Jonas Dantas Batista - involving the production, maintenance and/or use of animals belonging to the phylum Chordata, subphylum Vertebrata, for purposes of scientific research - is in accordance with the provisions of Law nº 11.794, of October 8th, 2008, of Decree nº 6.899 of July 15th, 2009, and the rules issued by the National Council for Control of Animal Experimentation (CONCEA) and it was approved for ETHICS COMMISSION ON ANIMAL USE (CEUA) from FEDERAL UNIVERSITY OF UBERLÂNDIA, in meeting of February 23rd, 2018).

| | |
|---|---|
| Vigência do Projeto | Início: 02/04/2018 Término: 30/01/2019 |
| Espécie / Linhagem / Grupos Taxonômicos | Rato heterogênico |
| Número de animais | 75 |
| Peso / Idade | 150-250 g / 8 a 10 semanas |
| Sexo | Machos |
| Origem / Local | Centro de Bioterismo e Experimentação Animal – CBEA – UFU |
| Número da Autorização SISBIO | - |
| Atividade(s) | - |

Uberlândia, 16 de março de 2018.